J|A|C|S ARTICLES

Published on Web 03/12/2010

Phase-Equilibrium-Dominated Vapor−Liquid−Solid Growth Mechanism

Chengyu He, Xizhang Wang, Qiang Wu, Zheng Hu,* Yanwen Ma, Jijiang Fu, and Yi Chen

Key Laboratory of Mesoscopic Chemistry of MOE and Jiangsu Provincial Laboratory for Nanotechnology, School of Chemistry and Chemical Engineering, Nanjing University, Nanjing 210093, People's Republic of China

Received December 25, 2009; E-mail: zhenghu@nju.edu.cn

Abstract: The vapor−liquid−solid (VLS) growth model has been widely used to direct the growth of one-dimensional (1D) nanomaterials, but the origin of the proposed process has not been experimentally confirmed. Here we report the experimental evidence of the origin of VLS growth. $Al_{69}Ni_{31}$ alloyed particles are used as "catalysts" for growing AlN nanowires by nitridation reaction in N_2-NH_3 at different temperatures. The nanowire growth occurs following the emergence of the catalyst droplets as revealed by in situ X-ray diffraction and thermal analysis. The physicochemical process involved has been elucidated by quantitative analysis on the evolution of the lattice parameters and relative contents of the nitridation products. These direct experimental results reveal that VLS growth of AlN nanowires is dominated by the phase equilibrium of the Al−Ni alloy catalyst. The in-depth insight into the VLS mechanism indicates the general validity of this growth model and may facilitate the rational design and controllable growth of 1D nanomaterials according to the corresponding phase diagrams.

Introduction

Vapor−liquid−solid (VLS) growth, first proposed in 1960s for whiskers growth,[1] is now being widely used to synthesize a large variety of one-dimensional (1D) nanomaterials.[2−4] This method works at elevated temperature, at which the liquid catalyst dissociates the vapor precursor and absorbs the species that can be alloyed with the catalyst. The resulting supersaturation then supports the whisker-like growth at the liquid−solid interface in a manner that minimizes the interface energy. In such a proposed model, the liquid catalyst seems to act as a medium for transporting species from the vapor phase to the whisker-like solid product. In studies of the last 40 years, the insight into the growth mechanism has been a lasting and crucial issue due to the importance of rationally controlling the compositions, sizes, crystal structures, and growth directions of the products. Upon the innovation of microscopy techniques, the overall VLS growth process has been observed phenomenologically by in situ transmission electron microscopy (TEM),[5−10] and the quantitative study on the kinetics of nucleation and growth of individual nanowires becomes feasible.[7−12] Very recently, scientists have tried to deeply understand VLS growth from the fundamental viewpoint of phase equilibrium by explaining the involved physicochemical process with the corresponding phase diagram of the alloy drops at the tips of nanowires.[13−17] Despite this progress, the intrinsic correlation between VLS growth and the phase equilibrium has not been established, which is actually the key in supporting this mechanism.

In our studies of 1D nanomaterials of compounds, we have extended the traditional VLS growth via introducing alloyed particles as "catalysts".[18] And the molten alloy catalyst here acts not only as the transport medium, as in the case of the traditional VLS growth, but also as the source to supply partial constituents of the final product.[19] This approach provides us a quite suitable alternate for the experimental exploration of the VLS mechanism by monitoring the evolution of the alloy catalyst and the nanowire products as well as the correlation between them. In this study, $Al_{69}Ni_{31}$ alloyed particles are used

(1) Wagner, R. S.; Ellis, W. C. *Appl. Phys. Lett.* **1964**, *4*, 89–90.
(2) Morales, A. M.; Lieber, C. M. *Science* **1998**, *279*, 208–211.
(3) Duan, X. F.; Lieber, C. M. *Adv. Mater.* **2000**, *12*, 298–302.
(4) Xia, Y. N.; Yang, P. D.; Sun, Y. G.; Wu, Y. Y.; Mayers, B.; Gates, B.; Yin, Y. D.; Kim, F.; Yan, H. Q. *Adv. Mater.* **2003**, *15*, 353–389.
(5) Wu, Y. Y.; Yang, P. D. *J. Am. Chem. Soc.* **2001**, *123*, 3165–3166.
(6) Stach, E. A.; Pauzauskie, P. J.; Kuykendall, T.; Goldberger, J.; He, R. R.; Yang, P. D. *Nano Lett.* **2003**, *3*, 867–869.
(7) Hannon, J. B.; Kodambaka, S.; Ross, F. M.; Tromp, R. M. *Nature* **2006**, *440*, 69–71.
(8) Kodambaka, S.; Tersoff, J.; Reuter, M. C.; Ross, F. M. *Phys. Rev. Lett.* **2006**, *96*, 096105.
(9) Hofmann, S.; Sharma, R.; Wirth, C. T.; Cervantes-Sodi, F.; Ducati, C.; Kasama, T.; Dunin-Borkowski, R. E.; Drucker, J.; Bennett, P.; Robertson, J. *Nat. Mater.* **2008**, *7*, 372–375.
(10) Kim, B. J.; Tersoff, J.; Kodambaka, S.; Reuter, M. C.; Stach, E. A.; Ross, F. M. *Science* **2008**, *322*, 1070–1073.
(11) Sutter, P. W.; Sutter, E. A. *Nat. Mater.* **2007**, *6*, 363–366.
(12) Eswaramoorthy, S. K.; Howe, J. M.; Muralidharan, G. *Science* **2007**, *318*, 1437–1440.
(13) Wang, Y. W.; Schmidt, V.; Senz, S.; Gösele, U. *Nat. Nanotechnol.* **2006**, *1*, 186–189.
(14) Kodambaka, S.; Tersoff, J.; Reuter, M. C.; Ross, F. M. *Science* **2007**, *316*, 729–732.
(15) Adhikari, H.; Marshall, A. F.; Goldthorpe, I. A.; Chidsey, C. E. D.; McIntyre, P. C. *ACS Nano* **2007**, *1*, 415–422.
(16) Sutter, E.; Sutter, P. *Nano Lett.* **2008**, *8*, 411–414.
(17) Kim, B. J.; Tersoff, J.; Wen, C. Y.; Reuter, M. C.; Stach, E. A.; Ross, F. M. *Phys. Rev. Lett.* **2009**, *103*, 155701.
(18) Huo, K. F.; Ma, Y. W.; Hu, Y. M.; Fu, J. J.; Lu, B.; Lu, Y. N.; Hu, Z.; Chen, Y. *Nanotechnology* **2005**, *16*, 2282–2287.

as the catalyst to prepare AlN nanowires via nitridation in N_2-NH_3 at different temperatures. By in situ analysis on the growth process and the precise characterization of the products, it is revealed that VLS growth of AlN nanowires follows the emergence of the liquid droplets of Al−Ni alloy catalyst and is dominated by the phase equilibrium of Al−Ni alloy. This study provides the experimental evidence for the origin of VLS growth, and the in-depth understanding of the VLS mechanism may facilitate the rational design and controllable growth of various 1D nanomaterials according to the corresponding phase diagrams.

Experimental Section

$Al_{69}Ni_{31}$ alloyed particles are used as the catalyst for the preparation of AlN nanowires by nitridation reaction in N_2-NH_3 (NH_3, 4 vol %) at different temperatures (see Supporting Information, Figures S1 and S2). In a typical run, the $Al_{69}Ni_{31}$ catalyst was placed in an alumina tube inside a horizontal tubular furnace. The chamber was flushed with argon several times to remove the oxygen and moisture and then heated to the desired temperature (e.g., 860, 900, 1000, 1100 °C) in argon. Subsequently, the argon was switched to N_2-NH_3 at a flow rate of 200 sccm, and the system was kept there for 2 h. The reactor was then cooled to ambient temperature in argon, and AlN nanowires were obtained.

Size distribution of the $Al_{69}Ni_{31}$ particles was examined by a particle size analyzer (Mastersizer 2000). The nitridation products were analyzed by scanning electron microscopy (SEM) (Hitachi S-4800), TEM (JEOLJEM-1005, 100 kV), high-resolution TEM (JEM-2010, 200 kV) equipped with an energy dispersive X-ray spectroscopy (EDS) detector, and X-ray diffraction (XRD) (Philips X'pert Pro X-ray diffractometer). The nitridation process was also examined by in situ XRD and thermogravimetry−differential scanning calorimetry (TG-DSC) (STA-499C thermal analyzer, Netzsch).

Results and Discussion

The morphological evolution of the products obtained by the nitridation reaction at several temperatures was observed by SEM as shown in Figure 1a−d (see Supporting Information, Figure S3).[20] No nanowires could be detected on the Al−Ni catalyst particles during processing at 840 °C (Figure 1a), while some short nanowires were found when the temperature was increased to 900 °C (Figure 1b). When the reaction temperature was raised to 1000 or 1100 °C, more nanowires grew out of the Al−Ni catalyst particles (Figure 1c,d). A typical TEM image for the product of 1000 or 1100 °C (Figure 1e) shows that the surface of the Al−Ni alloy catalyst was partially covered by the nanowires,[21] consistent with SEM observations (Figure 1c,d). EDS spectra suggest that the obtained nanowires are AlN, while the particle is the remaining catalyst composed of Al and Ni elements (Figure 1f). The C and Cu signals come from the copper grid, while the O signal from the unavoidable surface

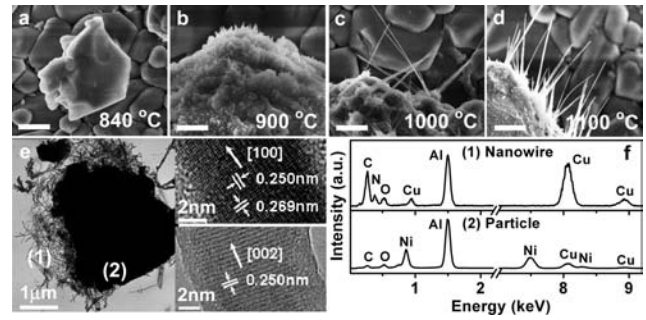

Figure 1. Morphological evolution of the nitridation products. (a−d) SEM images of the products obtained by nitriding the $Al_{69}Ni_{31}$ alloyed particles at 840, 900, 1000, and 1100 °C, respectively. No nanowires in the product of 840 °C (a), some short nanowires in the product of 900 °C (b), and more nanowires in the products of higher temperatures (c and d). Scale bar, 2 μm. (e) Typical TEM image for the products of 1000 or 1100 °C. Top inset: HRTEM image of a nanowire growing along [100] with spacings of 0.269 and 0.250 nm corresponding to d_{100} and d_{002} of h-AlN. Bottom inset: HRTEM image of a nanowire growing along [001] with spacing of 0.250 nm corresponding to d_{002} of h-AlN. (f) EDS spectra taken from sites (1) and (2) in (e), corresponding to the nanowires and particle, respectively. The obtained nanowires consist of Al and N elements, while the remaining catalyst particle is composed of Al and Ni elements.

oxidation of AlN.[22] Each AlN nanowire is a single crystal with the common growth direction of [100] or [001] (insets in Figure 1e), having a typical diameter around 20 nm and length up to micrometers.

To clarify the growth process of the AlN nanowires, the nitridation process of the $Al_{69}Ni_{31}$ alloyed particles was in situ examined in N_2 by TG-DSC from room temperature to 1200 °C with a rate of 10 °C/min. For comparison, the heating process of the $Al_{69}Ni_{31}$ particles was also examined by TG-DSC in inert Ar (Figure 2 and Supporting Information, Figure S4). For the case in Ar (Figure 2b), the DSC curve displays two endothermic peaks with onset temperatures of 853.9 and 1131.3 °C, resulting from the phase transition of the $Al_{69}Ni_{31}$ alloyed particles. This could be understood from the phase diagram of Al−Ni binary alloy shown in Figure 3,[23] where the vertical dashed line marks the composition of the $Al_{69}Ni_{31}$ alloy. Below 854 °C, the alloy is composed of two solid phases, i.e., Al_3Ni and δ (Al_3Ni_2), as confirmed by the XRD results (see Supporting Information, Figure S5). On heating across 854 °C (line ac), it experiences a phase transition from the region of Al_3Ni and δ phase into that of solid δ and liquid Al−Ni phase. On further heating across 1133 °C (line bd), it experiences the second phase transition into the region of solid β (AlNi) and liquid Al−Ni phase. So the two endothermic peaks in the DSC curve in Ar (Figure 2b) are attributed to the two phase transitions, respectively. No significant weight gain was observed in the corresponding TG curve in Figure 2b, as expected due to the inertness of Ar. For the case in N_2 (Figure 2a), besides the two similar endothermic peaks with the onset temperatures of 854.2 and 1130.2 °C arising from the phase transition, the DSC curve also shows an exothermic peak centered at 915.3 °C. This exothermic peak is accompanied by an obvious weight gain of about 7.2% in the TG curve in the range of 864.2−1100 °C, which is also reflected in the derivative thermogravimetry (DTG) curve, indicating the nitridation of the Al−Ni alloyed particles. We noted that the

(19) Strictly speaking, the alloyed particle is not a catalyst but rather a reactant, since it is partially consumed in the chemical reaction. In other words, a chemical reaction between the component(s) from the vapor precursor and the alloy "catalyst" itself takes place within the liquid "catalyst", and the resulting species precipitate in whisker-like morphology upon supersaturation.

(20) To learn the growth process of AlN nanowires on an individual particle, specimens for SEM measurement were prepared by nitrifying a spot of the $Al_{69}Ni_{31}$ particles on a flat alumina substrate, then directly moved to the SEM chamber for observation.

(21) The product in Figure 1e was prepared by nitrifying a mass of the $Al_{69}Ni_{31}$ alloyed powder in an alumina tube. To maintain its original shape to the greatest extent, the specimen for TEM measurement was obtained by dispersing the product into ethanol without ultrasonic treatment and then transferred onto carbon-coated copper grids.

(22) Wu, Q.; Hu, Z.; Wang, X. Z.; Lu, Y. N.; Chen, X.; Xu, H.; Chen, Y. *J. Am. Chem. Soc.* **2003**, *125*, 10176–10177.

(23) Massalski, T. B., Okamoto, H., Subramanian, P. R., Kacprzak, L., Eds. *Binary Alloy Phase Diagrams*, 2nd ed.; ASM International: Materials Park, OH, 1990; Vol. 1, p 183.

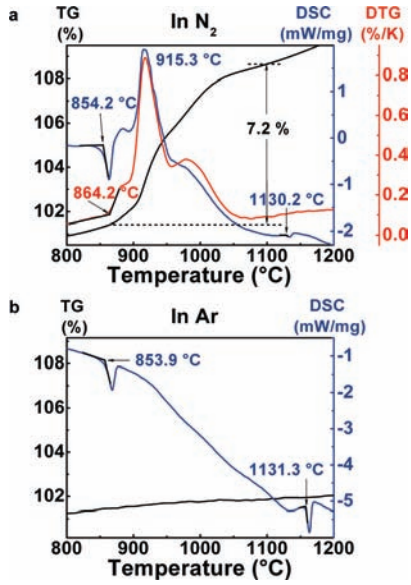

Figure 2. Thermal analysis of the $Al_{69}Ni_{31}$ alloyed particles. (a, b) TG(DTG)-DSC curves of the $Al_{69}Ni_{31}$ alloyed particles in N_2 and Ar, respectively. The DSC curve in N_2 or Ar displays two endothermic peaks near the phase-transition temperatures of 854 and 1133 °C of the $Al_{69}Ni_{31}$ alloy. The TG curve in inert Ar shows a featureless line (b) but an obvious weight gain of about 7.2% in N_2 in the range 864.2−1100 °C accompanied by an exothermic peak centered at 915.3 °C (a).

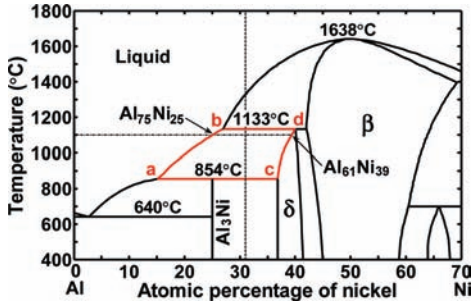

Figure 3. Al−Ni binary alloy phase diagram (data from ref 23). The vertical dashed line marks the composition of the $Al_{69}Ni_{31}$ alloy. For the $Al_{69}Ni_{31}$ alloy, phase transitions exist at 854 (line ac) and 1133 °C (line bd). The alloy is composed of the solid Al_3Ni and solid δ phases below 854 °C and the liquid Al−Ni and solid β phases above 1133 °C. In the range 854−1133 °C, the liquid Al−Ni and solid δ phases coexist and change along liquidus ab and solidus cd, respectively. The ideal formula of δ and β phase is Al_3Ni_2 and AlNi, respectively. At 1100 °C, the corresponding compositions of the liquid and solid phases are $Al_{75}Ni_{25}$ and $Al_{61}Ni_{39}$.

nitridation process resulting in the exothermic peak and weight gain followed the first phase transition, i.e., the appearance of the liquid Al−Ni alloy. This is further supported by the in situ XRD analysis of the nitridation process of the $Al_{69}Ni_{31}$ alloyed particles, which indicates that AlN species begin to form around 860 °C (see Supporting Information, Figure S5). These results suggest the intrinsic correlation between the growth of AlN nanowires and the formation of the Al−Ni alloy droplets; that is, the formation of the catalyst droplets (Al−Ni) is a precondition for VLS growth of 1D nanostructures (AlN).

The above analysis on the growth process is in nice agreement with the morphological evolution of the products in Figure 1a−d. Below 854 °C, only solid Al−Ni alloyed particles work as the catalyst, and it is argued that in such a case the nitridation is negligible. Accordingly no AlN nanowires could be formed in the product of 840 °C (Figure 1a). As the reaction temperature is above 854 °C, in addition to the solid δ phase, the liquid Al−Ni phase appeared (Figures 2 and 3). When N_2−NH_3 was introduced, reactive nitrogen atoms were produced on the surface of the Al−Ni catalyst droplets (Ni is a well-known catalyst for the dissociation of NH_3 and N_2),[24] leading to the formation of AlN species. With the accumulation of the AlN species, it precipitated into 1D geometry along the direction with minimized liquid−solid interface energy upon supersaturation. According to the phase diagram (Figure 3) and the lever rule, the relative amount of liquid Al−Ni phase increases with increasing temperature. Hence more AlN nanowires were formed with increasing reaction temperature, as demonstrated in Figure 1a−d (see Supporting Information, Figure S6).

To get a deeper insight into the physicochemical process involved in the growth, high-resolution XRD spectra were examined for the products prepared at 840, 860, 900, 1000, and 1100 °C, respectively, as shown in Figure 4. The XRD pattern for the product of 840 °C could be indexed to two phases of orthorhombic Al_3Ni (o-Al_3Ni) and hexagonal Al_3Ni_2 (h-Al_3Ni_2), identical to that for the reagent (see Supporting Information, Figure S1), indicating the stability of the $Al_{69}Ni_{31}$ alloyed particles at this temperature. For the products of 860−1100 °C, the diffraction peaks can be indexed to h-AlN and h-Al_3Ni_2. The former corresponds to the AlN nanowires, and the latter to the stable δ phase at the solidus cd in Figure 3, in agreement with the EDS analysis (Figure 1f). Moreover, from the local enlargement of the spectra, it is clearly seen that the three strongest lines of (100), (101), and (002) for h-AlN have negligible shift as anticipated (Figure 4b). In contrast, the three characteristic peaks of (001), (100), and (110) for h-Al_3Ni_2 have surprising progressive shifting toward the higher angles with increasing reaction temperature, with better resolution at the higher angle side (Figure 4c and Supporting Information, Figure S7). The lattice parameters *a* and *c* as well as the ratio of *c/a* for the δ phase were calculated from the XRD patterns (see Supporting Information, Table S1). Both *a* and *c* decrease precisely with increasing temperature, in agreement with the well-regulated up-shifting of the characteristic peaks, and the corresponding *c/a* ratio presents a monotonic increase, as plotted in Figure 4d (Supporting Information, Figure S7). As known, the integrated intensity of the diffraction peaks for an individual phase is proportional to its content in a mixture.[25] Here the integrated intensities for h-AlN and δ phases, denoted as I(h-AlN) and $I(\delta)$, respectively, were calculated for the products, and the ratios of I(h-AlN) to $I(\delta)$ are displayed in Figure 4e, which indicates a gradual increase of the relative amount of h-AlN with increasing temperature, in accordance with the SEM observation (Figure 1a−d). It is interesting to note that these quantitative experimental data from the XRD analyses on the nitridation products are in excellent agreement with the predictions derived from the rules of phase equilibrium.

From the phase diagram of Al−Ni binary alloy (Figure 3), it is clear that the liquid and solid phases coexist in the $Al_{69}Ni_{31}$ alloyed catalyst in the temperature range 854−1133 °C, and the composition of the solid δ phase changes along solidus cd, while that of the coexisting liquid Al−Ni phase along liquidus ab. Taking 1100 °C as an example, the compositions of the liquid and solid phases are $Al_{75}Ni_{25}$ and $Al_{61}Ni_{39}$, respectively. Shortly after introducing N_2−NH_3 gases, AlN nanowires started growing at the expense of the Al species in the liquid phase.

(24) Grunze, M.; Golze, M.; Driscoll, R. K.; Dowben, P. A. *J. Vac. Sci. Technol.* **1981**, *18*, 611–615.
(25) Jahanbagloo, I. C.; Zoltai, T. *Anal. Chem.* **1968**, *40*, 1739–1741.

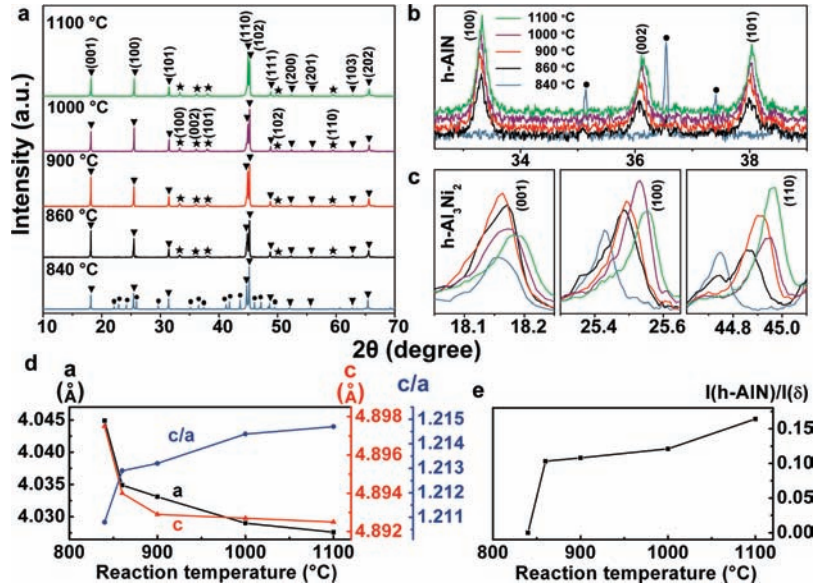

Figure 4. Quantitative XRD characterization of the nitridation products. (a) Survey XRD spectra of the products prepared at 840, 860, 900, 1000, and 1100 °C, respectively, with indicated (*hkl*) index for each peak. The products of 840 °C are indexed to o-Al_3Ni and h-Al_3Ni_2, and the products of 860−1100 °C to h-AlN and h-Al_3Ni_2. The peaks marked with a triangle (▲), pentagram (★), and solid circle (●) correspond to h-Al_3Ni_2, h-AlN, and o-Al_3Ni, respectively. (b) Local enlargement of the region containing the (100), (101), and (002) peaks of h-AlN with negligible peak shift for the products of different temperatures. For the product of 840 °C, the peaks marked with a solid circle come from o-Al_3Ni, and no AlN could be detected. (c) Local enlargement of the region containing the (001), (100), and (110) peaks of h-Al_3Ni_2 showing the progressive up-shifting with increasing reaction temperature. The resolution for the peak separation is in the order of group (110) > (100) > (001), since XRD has better resolution at the higher angle side (Supporting Information, Figure S7). (d) Lattice parameters *a* and *c* of the δ phase as well as the ratio of *c*/*a* versus the reaction temperature. *a* and *c* decrease, while *c*/*a* increases monotonically with increasing temperature. (e) The ratio of I(h-AlN)/$I(\delta)$ versus the reaction temperature. The plot indicates an increase of the relative amount of h-AlN nanowires with increasing temperature.

The gradual consumption of the Al species in the liquid phase resulted in a corresponding right shift of the system point. Meanwhile, to keep the compositions of the liquid and solid phases unchanged at this temperature, which is dominated by the phase equilibrium, partial Al−Ni in the liquid phase would transform to the solid phase, and the relative amount of the liquid and solid phase changed following the lever rule. The nitridation process concluded finally upon the disappearance of the liquid phase. Along this line, one can estimate that by the end of nitridation about 48% Al species in the initial liquid phase was consumed in the formation of AlN nanowires, while the remaining Al and all the Ni species were solidified to the $Al_{61}Ni_{39}$ phase (see Supporting Information S7). It has been calculated that the weight gain resulting from the nitridation reaction is about 7.8%, in agreement with the data measured by TG (Figure 2a).

Briefly, the above process could be schematically expressed as below:

$$Al_{69}Ni_{31}(s) \xrightarrow{1100\ ^\circ C} Al_{75}Ni_{25}(l) + Al_{61}Ni_{39}(s) \quad (1)$$

$$Al_{75}Ni_{25}(l) \xrightarrow{N_2\text{-}NH_3,\ 1100\ ^\circ C} \begin{cases} \rightarrow AlN(nanowires) & (2) \\ \rightarrow Al_{61}Ni_{39}(s) & (3) \end{cases}$$

Route 1 mentions the coexistence of $Al_{75}Ni_{25}$(l) and $Al_{61}Ni_{39}$(s) in the catalyst at 1100 °C. Upon introducing N_2-NH_3 at this temperature, routes 2 and 3 occurred simultaneously, and finally 48% Al species in $Al_{75}Ni_{25}$(l) is nitrified to produce AlN nanowire (route 2), and 52% Al and all the Ni species in $Al_{75}Ni_{25}$(l) are solidified to form $Al_{61}Ni_{39}$(s) (route 3). Here l and s represent liquid and solid phase, respectively.

As depicted by the solidus cd in Figure 3, the atomic ratio of Al/Ni in the solid δ (h-Al_3Ni_2) phase decreases with increasing temperature in the range 854−1133 °C. Consequently, more Al species will be nitrified into h-AlN nanowires with increasing temperature in this range, and the relative ratio of I(h-AlN)/$I(\delta)$ in the XRD pattern will increase accordingly. Furthermore, with decreasing Al/Ni ratio in the solid δ phase, both lattice parameters *a* and *c* of the δ phase should decrease due to the smaller atomic radius of Ni (1.62 Å) than that of Al (1.82 Å) and the ratio of *c*/*a* increases, which was well established in the literature in the studies on Al−Ni alloy (see Supporting Information, Figure S8).[26,27] All these expectations are in quantitative agreement with our experimental results shown in Figure 4d,e (see Supporting Information, Figure S7).

On the basis of the preceding quantitative XRD characterization on the nitridation products, the in situ TG-DSC and XRD analysis on the nitridation process, and the SEM observation on the morphological evolution of the nitridation products, it is revealed that VLS growth of AlN nanowires is actually dominated by the phase equilibrium of the Al−Ni alloy catalyst. The formation of the liquid catalyst droplets is the precondition for the growth of 1D nanostructures in a VLS manner. These conclusions have been further supported by the following supplemental experiments. The nitridation of the $Al_{69}Ni_{31}$ alloyed catalyst at a higher temperature of 1400 °C gives the product of cubic AlNi (c-AlNi) besides h-AlN nanowires (see Supporting Information, Figure S9), while no AlN nanowires can be formed by the nitridation of $Al_{50}Ni_{50}$ alloyed catalyst at 1100 °C (see Supporting Information, Figure S10) due to the absence of the molten catalyst droplets at this temperature

(26) Lu, S. S.; Huang, S. M.; Fu, C. M. *Acta Phys. Sin.* **1966**, *22*, 659–668.
(27) Bradley, A. J.; Taylor, A. *Proc. R. Soc. A* **1937**, *159*, 0056−0072.

(Figure 3), as required by the phase-equilibrium-dominated growth mechanism.

To the best of our knowledge, to date the mechanism-related studies on VLS growth remain restrictively in elemental nanowires especially Si and Ge nanowires[5,7−10,13−16] with little about compound nanowires known.[6] In this study, AlN compound nanowires have been synthesized by VLS growth, which is experimentally confirmed to be dominated by the phase equilibrium of Al−Ni alloy. The direct experimental evidence provides an in-depth understanding of the physicochemical process involved in the VLS growth and substantiates the general validity of the VLS mechanism, which has been widely applied for synthesizing various whiskers or 1D nanomaterials for over 40 years[1−4] but is not yet completely understood.[5−17]

Conclusion

In conclusion, extended VLS growth has been used to synthesize AlN nanowires by nitrifying $Al_{69}Ni_{31}$ catalyst particles with a gas mixture of N_2-NH_3 at different temperatures. This new approach provides an excellent model to experimentally elucidate the VLS mechanism. The whole nitridation process, which has been first examined by in situ TG-DSC and XRD, clearly reveals the direct correlation between the emergence of liquid droplets and the subsequent growth of nanowires. The physicochemical process involved in this VLS growth has been further illustrated in detail by quantitative analysis on the evolution of the lattice parameters and relative contents of the nitridation products. This direct experimental evidence unambiguously demonstrates that VLS growth of the AlN nanowires is actually dominated by the phase equilibrium of Al−Ni alloy catalyst. The in-depth insight into the growth process indicates the general validity of the VLS mechanism, which is of great importance in facilitating the rational design and controllable growth of various 1D nanomaterials according to the corresponding phase diagrams.

Acknowledgment. This work was jointly supported by the NSFC (20525312, 20833002, 20873057), "973" programs (2007CB936300), and the program for Changjiang Scholars and Innovative Research Team in University (PCSIRT). Z.H. thanks Dr. Lijun Yang for help with graphic drawings and valuable discussions.

Supporting Information Available: (1) Morphology, size distribution, and phase compositions of the $Al_{69}Ni_{31}$ alloyed particles; (2) TEM and SEM images of the nitridation products for the $Al_{69}Ni_{31}$ alloyed particles; (3) in situ TG(DTG)-DSC examination of the heating process of the $Al_{69}Ni_{31}$ alloyed particles; (4) in situ XRD analysis of the heating process of the $Al_{69}Ni_{31}$ alloyed particles; (5) schematic illustration of the nitridation process of $Al_{69}Ni_{31}$ alloyed particles for the growth of AlN nanowires; (6) detailed XRD analysis of the nitridation products; (7) weight-gain calculation for the nitridation of $Al_{69}Ni_{31}$ alloyed particles at 1100 °C; (8) nitridation of $Al_{69}Ni_{31}$ alloyed particles at 1400 °C; (9) nitridation of $Al_{50}Ni_{50}$ alloyed particles at 1100 °C. This material is available free of charge via the Internet at http://pubs.acs.org.

JA910874X